# **Automatic Focus Control of Charged-Particle Beams**

Abstract: The focusing mechanism for charged-particle beams is analyzed and its mathematical model is derived. Two control concepts for focusing electron beams are shown and the details of the feedback system for automatic focus control in the electron-beam recorder of an IBM photo-digital mass storage system are described (Fig. 9). Included are a representation of the mathematical system and the computer simulation results obtained from the digital simulation program DSL/90.

#### Introduction

Automatic focusing of electron beams and other chargedparticle beams has become a necessity in applications where consistently high resolution has to be achieved without human intervention. This paper describes such a system for precise and fully automatic control.

For an electron-beam recorder<sup>1</sup> having a beam diameter of about one micron and designed to operate essentially unattended, it was necessary to devise a fully automatic system for focusing the beam on the target. Two control-system concepts, both feasible for the recorder, are described in this paper. The one actually implemented is reported in detail, beginning with the mathematical representation of the mechanism involved in focusing the beam, and concluding with a digital system simulation. This nonlinear and time-varying system is one of several feedback systems used to accomplish stable and reliable control of the electron-beam column.<sup>2,3</sup>

Though physically different from electron beams, certain other charged-particle beams behave similarly (i.e., similar transducers and actuators can be used) and so conceivably can be focused by automatic means.

# Geometrical and physical considerations in focusing

The final portion of an image-forming system with circular symmetry can generally be represented by a simple diagram such as Fig. 1, which establishes the basic geometric relationship needed to formulate the mechanism of focusing. An essentially conical beam emerges from the system with its apex in the vicinity of a target, and an actuator, such as an electromagnetic lens, controls the axial position of the final crossover point and thereby the spot size (i.e., beam diameter in the target plane). A certain lens current  $I = I_0$  causes the beam to focus precisely on the target. For  $I < I_0$ , focus occurs at a distance z beyond the target,

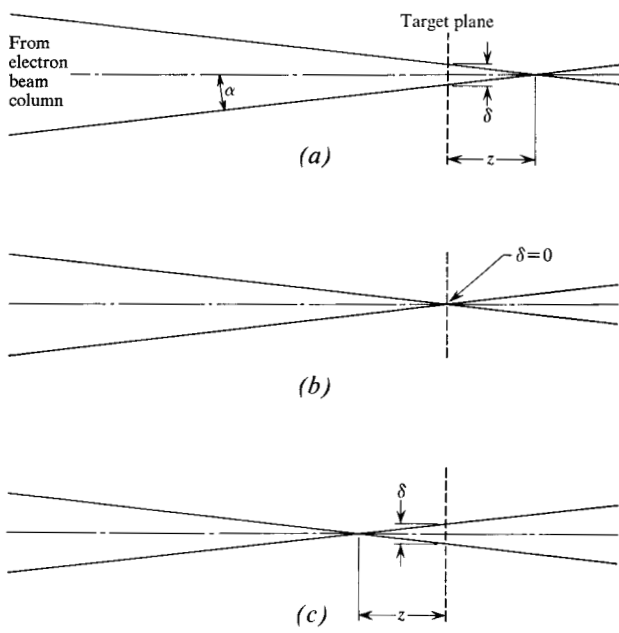


Figure 1 Geometry of a beam during focusing. (a) out of focus  $(I < I_0)$ ; (b) in focus  $(I = I_0)$ ; (c) out of focus  $(I > I_0)$ .

resulting in a spot size  $\delta$  in the target plane. Similarly, for  $I > I_0$ , focus occurs ahead of the target plane. For the typically very small beam semi-angle  $\alpha$ , therefore, the beam diameter is simply

$$\delta = 2\alpha z \,. \tag{1}$$

In the system considered here, focusing is achieved with a main lens of constant excitation and a smaller focus control lens which is used to correct small deviations from the desired position of the final crossover point. Both lenses are assumed to be in close proximity but without signifi-

171

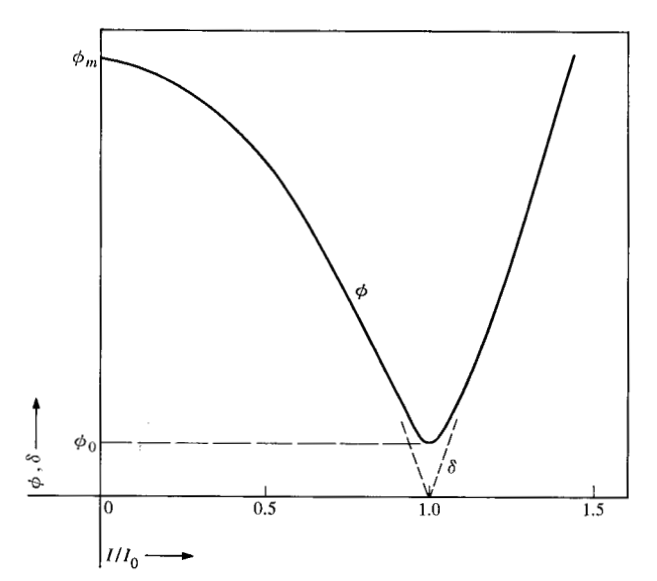


Figure 2 Spot size vs lens current.

cant overlap of their fields. Using the weak-lens approximation,<sup>4</sup> one obtains the relationship

$$z = k(1 - (I^2/I_0^2)), (2)$$

where k = const.

In addition, we can take into consideration that finite demagnification of the electron source and unavoidable aberrations cause the spot size  $\phi$  to be finite even at focus, namely  $\phi = \phi_0$ . The actual spot size  $\phi$  can then be approximated<sup>5</sup> by the relationship

$$\phi = (\phi_0^2 + \delta^2)^{1/2}, \tag{3}$$

where  $\delta$  is the spot size for the extreme case of  $\phi_0 = 0$ . A normalized expression of spot size versus lens current is obtained by combining Eqs. (1), (2), and (3):

$$\phi = \left[\phi_0^2 + C\left(1 - \frac{I^2}{I_0^2}\right)^2\right]^{1/2},\tag{4}$$

where  $C = 4\alpha^2 k^2$  is constant for the small focus corrections considered here.

Figure 2 shows a graph of  $\delta$  and  $\phi$  as functions of  $I/I_0$ , the lens current normalized with respect to the amount necessary to focus the beam in the target plane. Note that the expressions for spot size are independent of current polarity for this system, in which we have assumed negligible field overlap.

In Eq. (4), C can be interpreted as  $\phi_m^2 - \phi_0^2$ , where  $\phi_m = \phi$  (I = 0):

$$\phi = \left[\phi_0^2 + (\phi_m^2 - \phi_0^2) \left(1 - \frac{I^2}{I_0^2}\right)^2\right]^{1/2}.$$
 (5)

Thus an expression is derived that includes  $\phi_m$ , the local spot size maximum between the two minima obtained with different lens current polarities.

Figure 3 shows the realistic situation of a stationary target and varying distances of the coarse focal plane from it. These variations result in electron beam systems from such disturbances as cathode potential changes, lens current changes, and thermal expansion. For any given lens system,  $\phi_m$  and  $I_0$  are at all times quadratically related  $(\phi_m = KI_0^2)$ . The lens constant K can be determined from physical parameters of the lens system or experimentally obtained by means of  $\phi_m$  and  $I_0$  values from static  $\phi$  (I) curves.

After the interdependence of  $\phi_m$  and  $I_0$  is established through K, Eq. (5) for spot size  $\phi$  can be rewritten in the form  $\phi(I, K, \phi_0, \phi_m)$ :

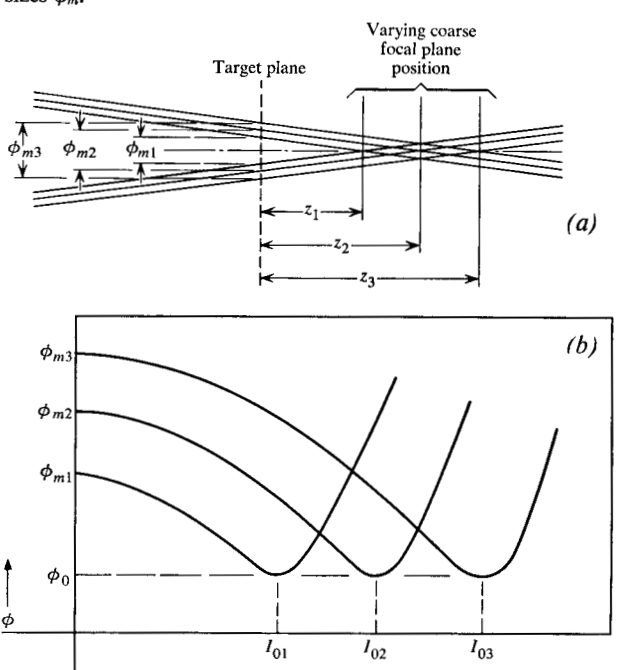
$$\phi = \left[\phi_0^2 + (\phi_m^2 - \phi_0^2) \left(1 - \frac{K}{\phi_m} I^2\right)^2\right]^{1/2}.$$
 (6)

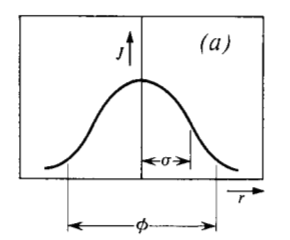
Figure 3 also shows a family of curves  $\phi(I)$  for three different  $\phi_m$  values, lens constant K, and constant  $\phi_0$ .

### **Transducer considerations**

Any feedback system for spot-size control must include a spot-size transducer, i.e., a device to measure the quantity to be controlled. Assuming the spatial distribution of electrons in the focused spot to be Gaussian in two dimensions and nearly circular, we can define the spot size  $\phi$  on the basis of a certain number of standard deviations  $\sigma$  (Fig. 4a).

Figure 3 Family of characteristic curves describing the physical mechanism of focusing a beam. (a) Illustration of shifts in coarse focal plane; (b) Spot size vs lens current for different initial spot sizes  $\phi_m$ .





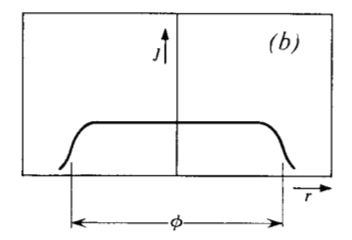


Figure 4 Current density distributions in the beam. (a) Distribution near focus; (b) distribution away from focus.

Though approximately valid near the focus point, the assumption of a Gaussian distribution is inaccurate elsewhere. The farther away from focus the beam current distribution is measured, the more uniform it becomes (Fig. 4b). Also, lacking instruments with suitable resolution, and lacking shape uniformity of the distribution function, spot size is not conveniently measured as a function of distance.

On the other hand, when the beam is scanned past a knife edge at constant speed, and the beam current is collected out of a detector placed beyond the knife edge, a signal can be conveniently generated that contains spot-size information. It exhibits a more or less rapid level change (depending on spot size) when the beam traverses the edge, as illustrated in Fig. 5. A relatively simple way of defining and measuring spot size is possible by analyzing the rise time of this signal, the target current  $I_T(t)$ . For instance, the 10\% and 90\% levels with respect to the maximum signal level (spot completely off the edge) can serve as the terminal points for the rise time  $t_r$ , and the time interval between the two points can be considered to be the time domain equivalent of spot size. If  $v_s$  is the scan velocity and  $t_r$  is the time interval between the 10\% and 90\% points, then the spot size is simply

$$\phi = v_s t_r . (7)$$

Since both scanning velocity and rise time are quite readily measured, spot-size determination becomes relatively easy for calibration purposes, as well as for control instrumentation. Unfortunately, contamination of the target edge and detector is a practical problem that limits application of the concept of scanning across a single knife edge. Therefore, we use an extension of this concept, scanning across a target with many edges which are equally spaced and close enough together to produce a train of roughly trapezoidal pulses. The rise and fall times of these pulses can then be repetitively measured and averaged to yield a continuous measure of spot size (Fig. 6).

# Control system concept

With an understanding of the focusing process and transducer capabilities, it becomes possible to develop a variety of feedback control-system concepts. One such concept

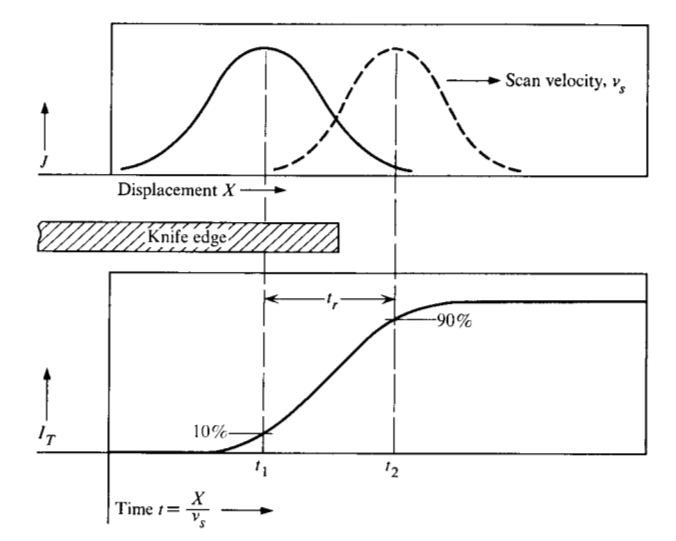
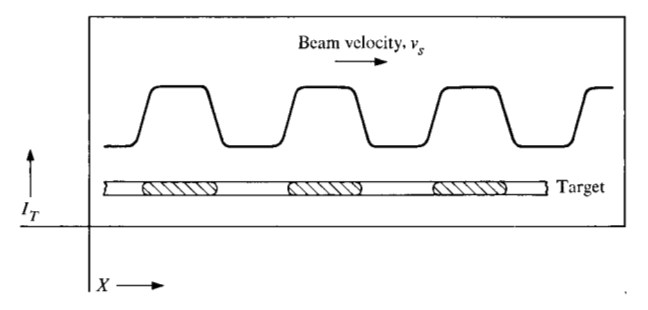


Figure 5 Spot-size determination through measurements in time domain.

Figure 6 Detector output vs beam position on test target.



was pursued and successfully implemented on the electronbeam recorder of the IBM Photo-Digital Mass Storage System.<sup>1</sup> The second concept is described in the section here entitled "Alternate Control Concept."

The main concept centered around the idea of building a system that can seek the lens current  $I_0$  that produces a minimum spot size  $\phi_0$ , regardless of its absolute value. The system was designed not to control the spot size in the target plane to a specified value but to produce the smallest spot size possible by precise focusing.

An opaque test target, containing a periodic hole pattern, is placed as accurately as possible in the plane of the specimen before a detector, so that the beam can be focused where it is needed to perform its task (e.g., exposure of photographic film) after the target is replaced by the specimen. Focusing the beam on this target, then, means finding the minimum spot size  $\phi$ , which is equivalent to finding the shortest rise time on the detector current trace.

Time differentiation of  $I_T(t)$  is an effective way of obtaining a signal related to spot size. As illustrated in Fig. 7,

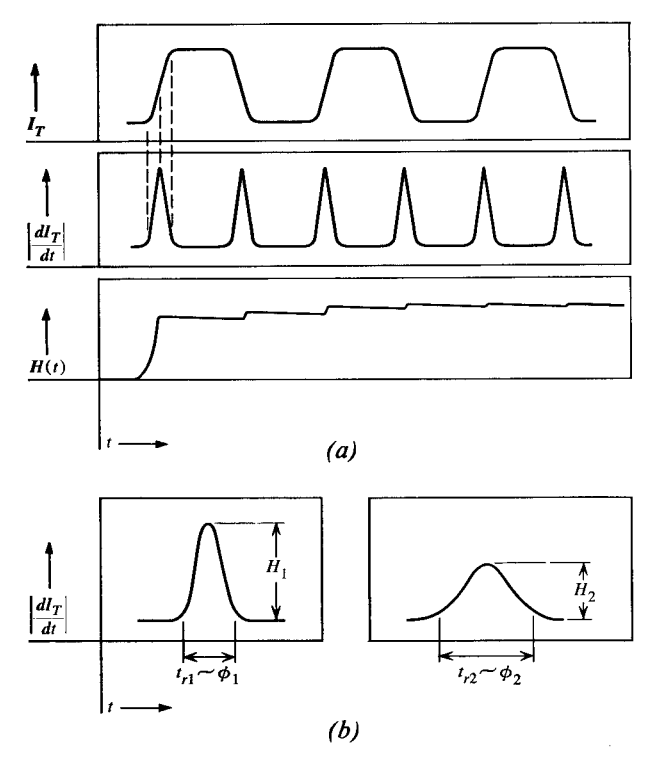


Figure 7 Extraction of a spot-size measure from the chopped-target current signal. (a) Generation of a continuous function  $H(t) \sim 1/\phi$  (t) by differentiation, rectification, and peak detection of  $I_T$ ; (b) interrelation of spot size and peak detector output.  $\phi_1 H_1 = \phi_2 H_2$ ;  $H\phi = \text{const}$ ;  $H \sim 1/\phi$ .

a train of impulses is obtained after differentiation and full-wave rectification of  $I_T(t)$ . This signal is used to generate a function  $H(t) \sim 1/\phi(t)$  by means of peak detection. Maximization of H as a function of current in the focus control lens  $I_{\rm FCL}$  is then equivalent to minimization of  $\phi(I_{\rm FCL})$ . Finding the peak of the  $H(I_{\rm FCL})$  curve, in turn, is equivalent to making its approximate derivative  $\epsilon = \Delta H/\Delta I_{\rm FCL}$  equal to zero (Fig. 8). To accomplish the latter, a square wave "dither" is superimposed on the lens current. The resulting oscillatory output of the rectifier is selectively switched into two peak detectors in synchronism with the dither. By this means, the finite difference is, in effect, taken of the  $H(I_{\rm FCL})$  curve with respect to lens current, as long as the dither amplitude remains constant.

During one dither half-period, one peak detector receives the rectifier output corresponding to the increased instantaneous lens current and generates the dc signal  $H_{\rm HI}$ . During the second half-period of the dither, the other peak detector receives the rectifier output, resulting in the dc signal  $H_{\rm LO}$ . An error signal  $\epsilon$ , as defined in Eq. (8), is then easily generated by means of a differential amplifier:

$$\epsilon = H_{\rm HI} - H_{\rm LO} = \Delta H \sim \frac{\Delta H}{\Delta I_{\rm ECL}}.$$
 (8)

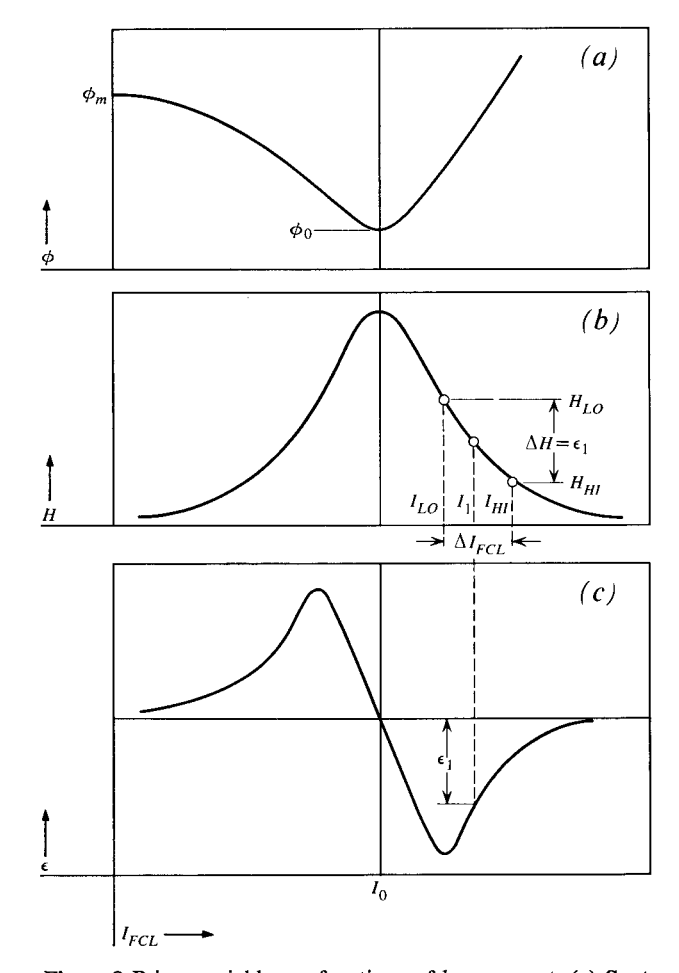


Figure 8 Prime variables as functions of lens current. (a) Spot size; (b) peak detector output; (c) error.

As shown in Fig. 8, the zero crossing of the error curve is essentially\* coincident with the  $I_0$  point of the  $\phi(I_{FCL})$  curve, which is the desired lens current that causes the beam to focus on the target.

Upon approximate integration with respect to time, the error is then used to increase or decrease the lens current in accordance with the error polarity in such a way as to focus the electron beam. A negative error causes the lens current to decrease and a positive error causes it to increase. The system gain is chosen that the zero error point is as stable as compatible with transient requirements.

Figure 9 shows the functional relationship of the various system components. The block following the integrator, labelled "analog store," has so far not been mentioned. This device provides the means for opening the system loop during the beam utilization periods for maintaining the lens-driver input voltage—similar to the conventional motor-driven potentiometer.

<sup>\*</sup> Note that  $\epsilon$  would be zero exactly at  $I_0$  if it were the differential quotient  $dH/dI_{\rm FCL}$ . But because  $\epsilon$  is the difference quotient  $\Delta H/\Delta I_{\rm FCL}$ , and because  $\phi$  and H are not perfectly symmetrical around  $I_0$ , there is a slight discrepancy between  $I_0$  and the zero crossing of  $\epsilon(I_{\rm FCL})$ .

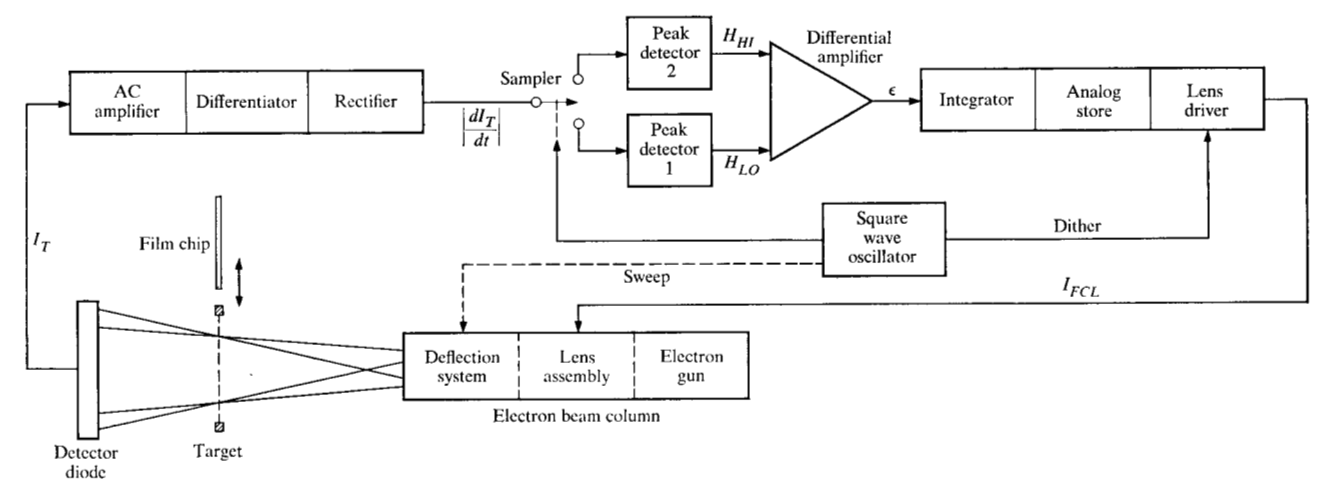


Figure 9 A focus control system for an electron beam device.

# Implementation of an electron-beam focus-control system

#### • Focus control lens

In the electron beam recorder of the photo-digital mass store, a small electromagnetic lens without pole pieces (150 ampere-turns) is placed just ahead of the final main lens which accomplishes the coarse focusing. (For a detailed description of the electron-beam system see Ref. 3.) With the selected lens materials and the particular geometry of the lens, a dynamic response time of less than 1 ms is achieved; i.e., as a consequence of a step current change in the coil, the beam shape change is accomplished exponentially with a time constant of about 250  $\mu$ s.

Because of its close proximity to the final main lens, the focus control lens field is coupled with the final lens field in such a way as not to be completely independent of current polarity in the focus control lens as initially assumed. Empirical data show that it requires 80 mA less current to focus the beam for one polarity than the other, characterized by a 40-mA shift of the symmetrical  $\phi(I_{\rm FCL})$  curve, as shown in Fig. 10.

Measurements of several pairs of  $(\phi_m, I_0)$  values for different coarse focus conditions yielded a value of  $350\mu/A^2$  for the characteristic number K of the lens, when the offset due to the final lens field was given due consideration. Using the favorable current polarity—that which requires less current—means that even small quantities of current have the effect of noticeably reducing the spot size. On the other hand, when the unfavorable current polarity is used, small quantities of lens current will increase the spot size (Fig. 10).

# • Target and detector

The transducer for spot-size measurement consists of an electroformed 0.5-mil nickel foil with a rectangular hole

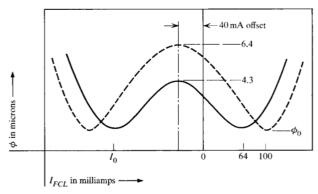
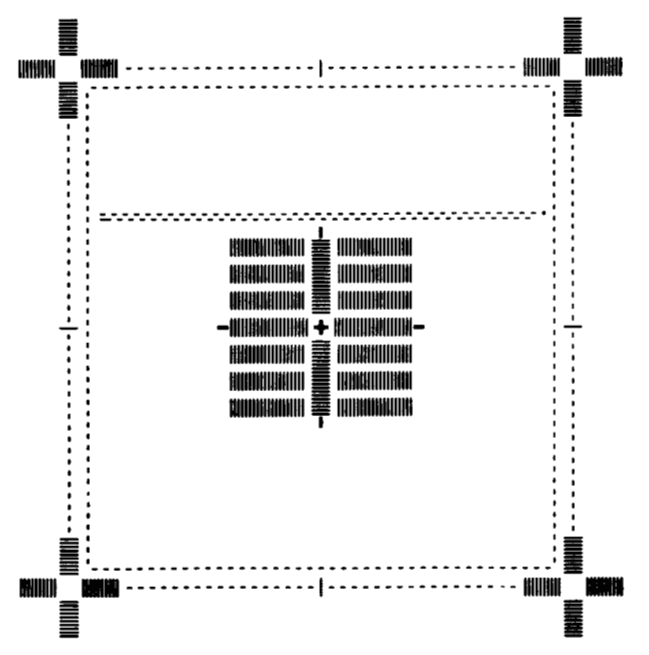


Figure 10 Measured spot size vs lens current.

Figure 11 Test target.



175

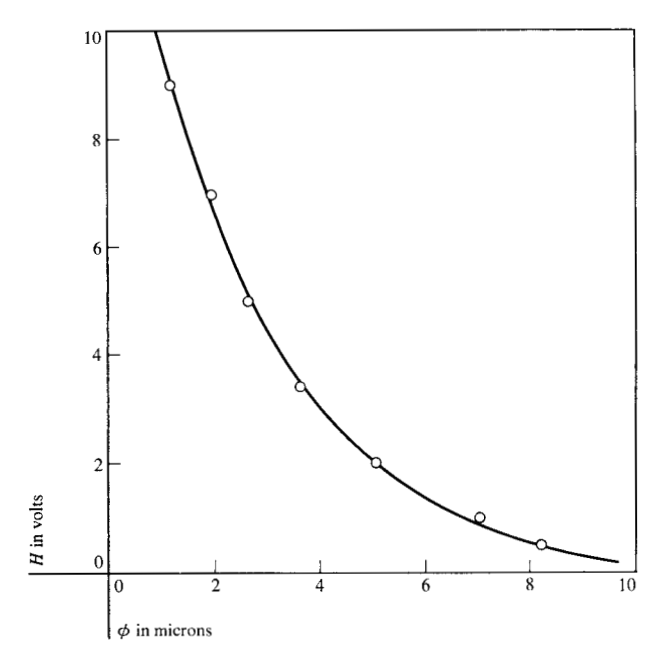


Figure 12 Measured peak detector output vs spot size.

pattern (Fig. 11), together with a p-n junction diode for direct electron-beam bombardment. Several sets of slots measuring 1  $\times$  10 mils are etched into the target at various places on and off axis. The slots are spaced at two-mil intervals and are arranged along orthogonal lines such that spot tests can be performed in two perpendicular directions, either one at a time or alternately. This scheme permits spot-size measurement in two dimensions. By deflecting the beam back and forth across a number of holes at a constant beam speed, a 2 kHz signal of trapezoidal wave shape is generated at the output of the diode (Fig. 6).

#### • Detection circuitry

The target current signal out of the diode is initially amplified to a level of two volts by an ac amplifier with a 10 Hz to 250 kHz bandwidth. In a separate servo system the target current level is regulated to 5 nA by utilizing the ac amplifier output as its feedback signal. A differentiator with a cut-off frequency of 200 kHz and unity gain at 2.5 kHz, followed by a full-wave rectifier, produces the 4 kHz train of impulses with bases directly proportional to spot size and with heights inversely proportional. Two peak detectors with charge time constants of about 100 µs and discharge (hold) time constants of 50 ms receive alternately bursts of impulses in synchronism with positive and negative half-cycles of the square-wave dither superimposed on the lens current. Dither (240 Hz square wave) and sweep (120 Hz triangular wave) are synchronized, since we found that low-frequency system oscillations (beating at the difference frequency of dither and sweep) were present when no synchronism existed. In addition, a set of delay circuits

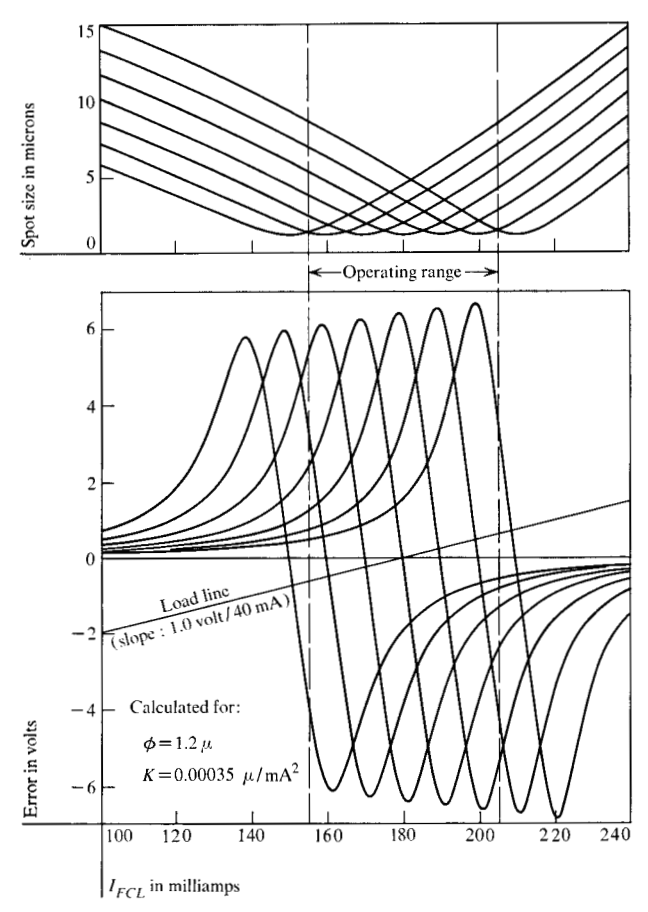


Figure 13 Characteristic curves calculated for realistic operating conditions. (Traces from automatic plotter chart.)

is used to blank out erroneous\* pulses immediately after each dither reversal, causing bursts of impulses to appear only about one-third of the time on the input of each peak detector.

Differencing of the two peak-detector output signals is accomplished by an operational differential amplifier with a 30-Hz bandwidth and 1.0 closed-loop gain. Its output, termed "error," is the quantity which determines the corrective action to be taken to focus the beam.

# • Drive circuitry

To guarantee the error to be zero or very nearly zero after servoing to steady state, an integrating element was placed in the forward path of the loop. Aside from its capability to filter the ripple in the differential amplifier output, its output can easily be seen to have the desirable property of reaching a constant value at steady state as the error nears zero. This final integrator output value, then, is the lens driver input voltage that corresponds to the required lens current  $I_0$  which focuses the beam at the given time. The integrator is a simple RC filter whose  $0.7 \mu F$  capacitor to

<sup>\*</sup> Erroneous, since eddy current losses in the lens prohibit instantaneous field response to dithered lens current.

ground is part of an analog storage element that is capable of holding a voltage constant over extended periods of time. A reed switch, located ahead of the capacitor, serves to close and open the loop for each focusing interval. A field-effect transistor, following the capacitor, effectively prevents leakage of the stored charge during hold periods.

The last element in the servo loop is the lens driver. Its inputs are a reference voltage, the servo voltage out of the analog storage element, and the dither; its load is the focus control coil. The reference voltage sets up the center of the operating range at 180 mA, the servo signal is designed to yield  $\pm$  25 mA servo current by way of a 40 mA/V lens driver gain, and the dither amplitude is  $\pm$  10 mA. A current response to the dither step disturbances of about 100  $\mu$ s settling time was achieved, making the lens driver sufficiently faster than the lens itself.

A total loop gain of 31.6  $\pm$  2.0 is obtained under the following conditions: unity dc gain in the differential amplifier and in the integrator; 40 mA/V in the lens driver; and a measured slope of 0.74 to 0.84 V/mA in the linear dynamic range of the error vs lens current curve, which represents lens and detection circuitry. For small errors this gain yields slightly underdamped response for the approximately linear second-order system whose open-loop poles are due to the integrator (700 ms) and the sample and hold circuit (13 ms).

#### System analysis

Construction of the characteristic curves for the system (in the realistic operating range of  $180 \pm 25$  mA lens current) is possible after obtaining the number K for the lens, and the relationship between peak detector output H and spot size (Fig. 12). Figure 13 displays a family of  $\phi$  ( $I_{FCL}$ ) curves calculated by means of Eq. (6) for  $\phi_0 = 1.2\mu$ , and the corresponding set of  $\epsilon(I_{FCL})$  curves obtained by the approximate relationship  $H = 12/\phi$  for a dither magnitude of 10 mA. This family of curves represents the lumped nonlinearity in the loop whose shape varies slightly from one end of the operating range to the other. A minor shape change is also to be expected from variations in minimum spot size  $\phi_0$ . As system parameters, like  $\phi_m$  and  $\phi_0$ , vary from one refocusing interval to the next, the control system must adapt itself to these changes and find the spot-size minimum.

Figure 14 shows, in block diagram form, the mathematical model of the system. Aside from two nonlinear functions discussed above, the diagram shows two other operational blocks. One is the difference operator  $\Delta/\Delta I_{\rm FCL}$ , representing the way in which  $\epsilon$  is obtained from H by using dither and the differential amplifier. The other is the linear transfer function between error and servo current. The latter is made up of three factors: the dc gain in the drive circuitry; the real pole due to the RC filter for approximate integration ( $\tau_2 = 700 \, {\rm ms}$ ); and a real pole due to the sampling process ( $\tau_1 = 13 \, {\rm ms}$ ), as obtained through frequency response tests.

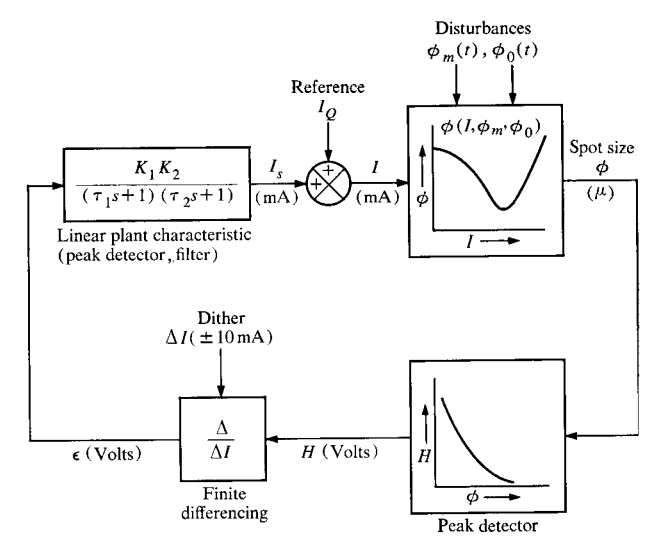
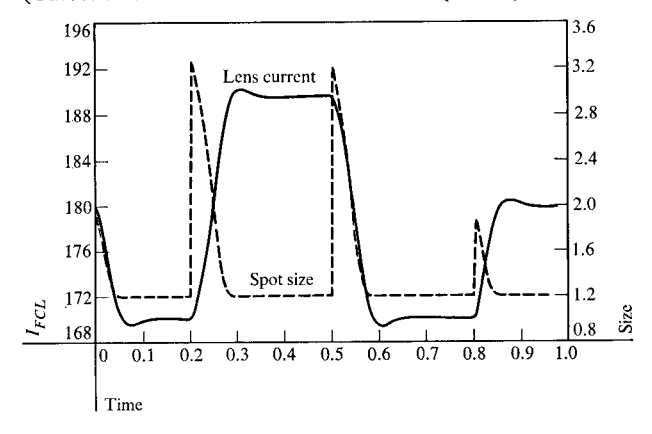


Figure 14 Mathematical model of the system.

$$K_1~K_2=40~\text{mA/V};~\tau_1=13~\text{ms},~\tau_2=700~\text{ms}.$$
  $\phi=\sqrt{\phi_0^2+(\phi_m^2-\phi_0^2)(1-I^2/I_0^2)^2}$   $I_0^2=\phi_m/K;~K=0.00035\mu/\text{mA}^2$ 

Figure 15 Step response obtained from DSL/90 program. (Curves traced from charts from automatic plotter.)



In the approximately linear vicinity of focus, where the loop gain is essentially constant, a linear model of second order holds, and the transient response can be easily estimated. Outside the linear zone, more exact methods of nonlinear analysis must be used to obtain transient response information. The IBM general purpose digital simulation program DSL/90 was used to simulate the system in its various design stages, aiding in design optimization and performance evaluation.<sup>6,7</sup> Figure 15 shows the transient response\* obtained from the simulation for step disturbances in the vicinity of the operating range center that

<sup>\*</sup> In Fig. 15 the independent variable  $I_{\rm FCL}$ , the current in the focus control lens in mA, is defined as  $I_L - 40$ ; and SIZE, the spot size in microns, is the variable name chosen for  $\phi$ .

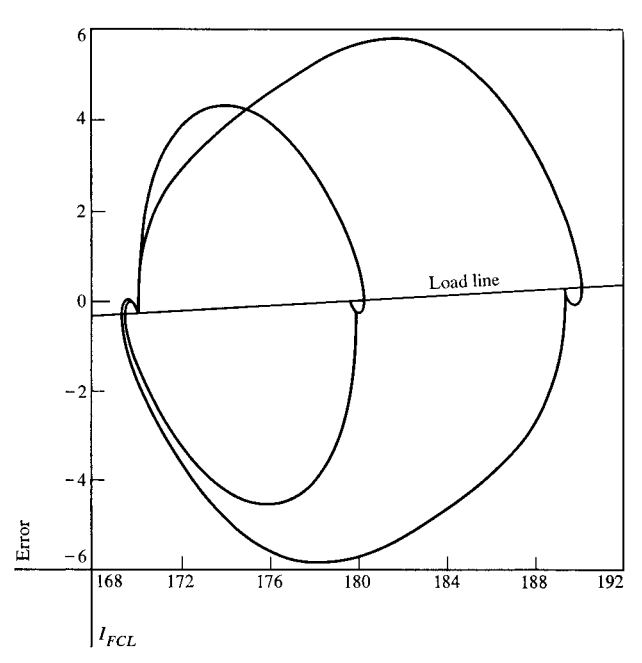


Figure 16 Phase-plane trajectories associated with the transient response curves of Figure 15.

correspond to 5 and 10 mA lens-current changes. The disturbances were introduced in the form of step changes in the parameter  $I_0$ , which is equivalent to changes of the basic spot size  $\phi_m$  regardless of cause. Even though slight overshoot in lens current is apparent, the spot size approaches its minimum without apparent bounce. The system is capable of focusing spots of initially 2  $\mu$  and 4  $\mu$  in diameter well within the desired time intervals of 200 ms and 500 ms, respectively. Experimentally obtained transients in response to step disturbances resembled closely those obtained by simulation, proving the validity of the mathematical model of the system.

As in any control system of Type 0 (without pure integrators), the steady-state error for step inputs is nonzero everywhere, except at the center of the operating range. A straight line with a slope of 1 V per 40 mA in the  $\epsilon$  ( $I_{\rm FCL}$ ) plane, intersecting the abscissa at  $I=I_Q=180$  mA (the quiescent current), is the locus of the operating points for the error signal. This locus is, in effect, the load line of the system (Fig. 13). Wherever a particular error curve intersects the load line, the system will come to rest, as can be seen by examining the phase plane trajectories ( $\epsilon$  vs  $I_{\rm FCL}$ ), shown in Fig. 16. Because the error curves are all very steep near their zero points and the spot size curves are quite flat, the operating points yield near-perfect focus, even at the extremes of the operating range.

## Alternate control concept

For applications where target removal and/or dithering of the lens current are to be avoided, a second control concept may be considered. Though similar to the one described above, it is in several ways superior, but inherently not quite as accurate. Figure 17 illustrates the essential aspects of the scheme.

In this system a target, offset to a distance z beyond the specimen, is used to focus the beam at the target by controlling the spot size at the target  $\phi$  to the constant value  $\phi_1 = 2\alpha z$ . Since the distance z remains constant, and the beam has a consistently conical envelope, the beam will be in focus at the specimen if the spot size at the target is kept constant at  $\phi_1$ . Requiring no minimization of H (the peak detector output), this concept allows operation without dither. Also, if the physical dimensions are such that z is large enough to separate target and specimen plane sufficiently, it makes possible the feature of a stationary test target beyond the specimen.

As shown in Fig. 17, a lens current  $I_1 > I_0$  is required to obtain a spot size  $\phi_1 > \phi_0$  in the target plane so that focus occurs at the specimen. A certain peak detector output value  $H_1$  then corresponds to the spot size  $\phi_1$  that must exist in the target plane at steady state. That nominal value  $H_1$  can be used as a reference voltage with which the instantaneous peak-detector output voltage is compared. The difference  $(H-H_1)$  can serve as the error signal for this system, requiring no finite differencing (i.e., dither and samples) as in the first concept but relying on good reference voltage regulation and calibration between  $\phi$  and H. The operating point would have to be located on the relatively linear part of the slope on the  $H(I_{\rm FGL})$  curve near the inflection point to optimize linearity and repeatibility from one curve to the next.

The concept was implemented on the electron-beam recorder and worked as expected: the transient response was significantly faster compared to that of the minimum-seeking system because the sampler time-constant was no longer in the loop. Higher stability existed (there being no overshoot and beating problem), and the operating range was potentially increased because of the open-ended error curve on the high-current side. The close spacing of the target with respect to the specimen plane in the given situation was, however, incompatible with the existing machine design, making the mechanical advantage of a stationary target unrealizable. The inherent variations in the absolute value of the minimum spot size, or maximum peak detector output, are of no concern, since the effects of these changes are felt only in the immediate vicinity of focus-not near the operating point—as indicated by the dashed lines in Fig. 17.

#### Summary

The mechanism involved in focusing a beam of charged particles, in particular an electron beam, has been reviewed, and analytic expressions have been derived relating spot size in the image plane to a number of variables and

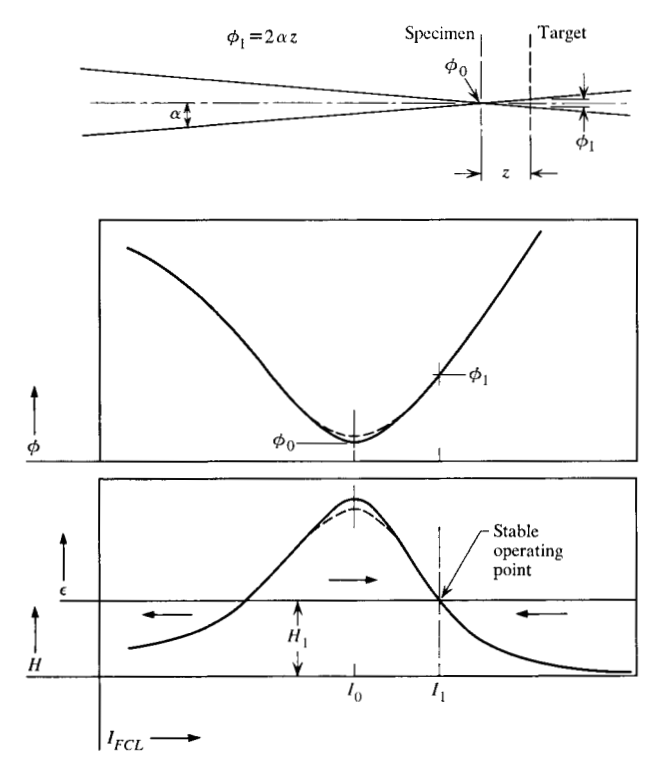


Figure 17 Alternate focusing concept.

parameters which influence it. Based on an understanding of the focusing problem in general and a suitable combination of actuator and transducer, two specific feedback control system design concepts are described, one of which is being used in the electron-beam recorder of an IBM photodigital mass storage system.

In view of the fact that the electron beam focus control system has been implemented and found to function well in the field, it can safely be stated that automatic focus control of charged particle beams is indeed feasible and practical. Comparison of test data with results obtained by digital simulation indicates that a valid mathematical model of the control system exists, permitting analytic studies of the present system as well as extensions for future efforts.

## **Acknowledgments**

The author expresses thanks and appreciation to Dr. Fred Kurzweil and Robert R. Barber, who initially formulated the control concept; to Dr. Karl H. Loeffler who advised in electron-optical matters; to Paul C. Lang and T. Jay Cameron, who were primarily responsible for circuit design, implementation and system testing; to Chiu H. Ting, who was instrumental in the transducer design; and to Dr. Joseph R. Werning, who directed the program for developing the electron beam column and control systems.

#### References

- J. D. Kuehler and H. R. Kerby, "A Photo-Digital Mass Storage System," Proceedings of the Fall Joint Computer Conference, pp. 735–742 (1966).
- F. Kurzweil, Jr., R. R. Barber, and M. H. Dost, "Automatic Control of an Electron Beam Column," *Proceedings of the IEEE 9th Annual Symposium on Electron, Ion and Laser Beam Technology*, pp. 350–362 (1967).
  K. H. Loeffler, "An Electron Beam System for Digital Re-
- K. H. Loeffler, "An Electron Beam System for Digital Recording," Proceedings of the IEEE 9th Annual Symposium on Electron, Ion and Laser Beam Technology, pp. 344–349 (1967).
- 4. P. Grivet, Electron Optics, Pergamon Press Ltd., p. 101, 1965.
- 5. Ibid., p. 423.
- M. H. Dost and R. R. Barber, "Simulation of Electron Beam Control Systems Using DSL/90," Simulation, pp. 237, 247 (November 1967).
- W. M. Syn and R. N. Linebarger, "DSL/90—A Digital Simulation Program for Continuous System Modeling," "Proceedings of the Spring Joint Computer Conference, pp. 165–187 (1966).

Received March 1, 1967.